

Thermal stability of a 4 meter primary reflector for the Scanning Microwave Limb Sounder

Richard E. Cofield^a and Eldon P. Kasl^b

^aJet Propulsion Laboratory (JPL), California Institute of Technology, 4800 Oak Grove Drive, Pasadena, CA 91109-8099, USA;

^bVanguard Space Technologies, 9431 Dowdy Drive, San Diego, CA 92126-4336, USA

ABSTRACT

The Scanning Microwave Limb Sounder (SMLS) is a space-borne heterodyne radiometer which will measure pressure, temperature and atmospheric constituents from thermal emission in [180,680] GHz. SMLS, planned for the NRC Decadal Survey's Global Atmospheric Composition Mission, uses a novel toric Cassegrain antenna to perform both elevation and azimuth scanning. This provides better horizontal and temporal resolution and coverage than were possible with elevation-only scanning in the two previous MLS satellite instruments. SMLS is diffraction-limited in the vertical plane but highly astigmatic in the horizontal (beam aspect ratio $\sim 1:20$). Nadir symmetry ensures that beam shape is nearly invariant over $\pm 65^\circ$ azimuth. A low-noise receiver FOV is swept over the reflector system by a small azimuth-scanning mirror. We describe the fabrication and thermal-stability test of a composite demonstration primary reflector, having full 4m height and 1/3 the width planned for flight. Using finite-element models of reflectors and structure, we evaluate thermal deformations and optical performance for 4 orbital environments and isothermal soak. We compare deformations with photogrammetric measurements made during soak tests in a chamber. The test temperature range exceeds predicted orbital ranges by large factors, implying in-orbit thermal stability of 0.21 micron rms/ $^\circ\text{C}$, which meets SMLS requirements.

Keywords: microwave limb sounding, composite reflectors, toroidal, thermal distortion, physical optics

1. INTRODUCTION

The Scanning Microwave Limb Sounder (SMLS) instrument, planned for launch aboard the Decadal Survey's Global Atmospheric Composition Mission (GACM), studies fast tropospheric processes using the microwave limb sounding technique, whose vertical resolution and cloud and aerosol penetration have already been demonstrated with current instruments (UARS and Aura MLS). While daily vertical profile observations from these satellite instruments have provided needed first-order information on the upper troposphere, they lack the spatial and temporal resolution required to quantify important smaller-scale processes that dominate this region's behavior on larger scales from regional to global.

The toric Cassegrain antenna developed for SMLS¹ provides azimuth-independent scanning over a $\pm 65^\circ$ swath of a conical scan (about the nadir axis) from an 830 km orbit (Fig. 1a). Fig. 1b shows the accommodation of SMLS on a conceptual GACM spacecraft. Primary, secondary and tertiary surfaces of the antenna are generated by rotating conic sections about a common toric axis in the nadir direction. Proper choice of the conic foci and the toric axis transforms a feed pattern with circular symmetry into a very narrow vertical illumination of the primary (Fig. 1c). The resulting far-field pattern is diffraction limited in the limb vertical direction and $\sim 20\times$ broader, independent of azimuth, in the horizontal. A small (~ 10 cm diameter) mirror scans the beam over the antenna, while a slower $\sim 2^\circ$ nod of the entire antenna provides the vertical scan. The resulting scan pattern benefits Earth science by providing dramatic improvements in temporal and spatial (lateral) resolution and coverage, which will propagate to the body of atmospheric science and become available for policy decisions pertaining to climate change and pollutant transport.

Further author information: (Send correspondence to R.E.Cofield)

R.E.Cofield: E-mail: Richard.E.Cofield@jpl.nasa.gov, Telephone: (818) 354-2501, Fax: (818) 393-5065

E.P.Kasl: E-mail: ekasl@vanguardcomposites.com

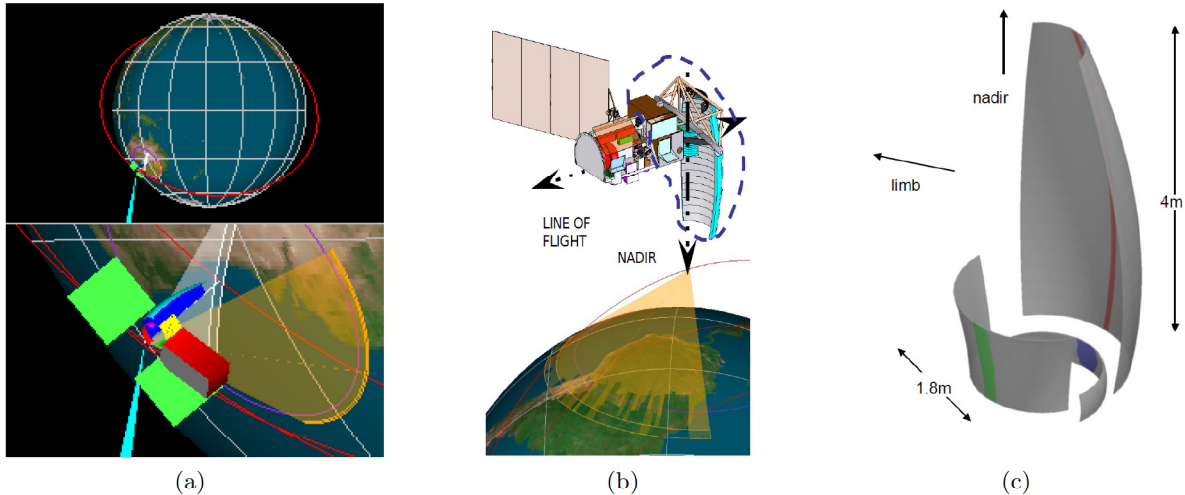


Figure 1. SMLS antenna: (a) view from Sun in 830 km, $I = 52^\circ$ inclination orbit at the time of worst-case solar heat load on Primary Reflector (b) accommodation on GACM spacecraft; and (c) reflector illumination for a single azimuth pixel.

In a recent study we demonstrated thermal stability of a 4 meter primary reflector for the toric Cassegrain antenna of SMLS in the GACM orbit. We built a graphite fiber reinforced composite panel of size 4m x (1/3 width of flight SMLS), which provides full diffraction-limited performance of the center pixels of GACM SMLS. The reflector fabrication used a mold made in phase II of a NASA Small Business Innovative Research (SBIR) program by Vanguard Space Technologies, Inc.² The thermal stability test was developed from similar tests of communications antennas (C to Ka bands) to verify figure performance under flight-like thermal soak environments using photogrammetric measurements.

This paper describes the application of the toric Cassegrain design¹ to GACM SMLS and the mathematical models used to predict its optical performance in both the candidate GACM orbits (for the full-size SMLS) and in thermal soak test of the demonstration reflector. We present preliminary results of a current research program in which we revisit those test results to correlate model predictions and extend them to planned thermal gradient tests of both the 1/3 and full-width primary reflectors in a large controlled test facility. We shall also use modeled antenna patterns in geophysical parameter retrieval simulations to specify performance based on GACM science requirements.

2. DESIGN AND ANALYSIS

Major changes in the SMLS antenna since its first design study¹ are: increase of orbit altitude from 705 to 830 km, doubling of the vertical aperture, from 1.6 to 3.2 m (4 m reflector height projected on a plane normal to the limb direction), and extension of the azimuth range to $\pm 65^\circ$. Nevertheless, the toric design procedure was followed as before to define a configuration compatible with the GACM spacecraft and launch vehicle concepts. The large antenna size and wide range of sun angles in these concepts preclude a sun shade. Therefore, optical performance in the thermal environment of Low Earth Orbit must be studied carefully to assure that science requirements for SMLS will be met, as they were for the previous UARS and Aura MLS instruments which observed similar frequencies in similar orbits.

A key parameter in the thermal balance of Earth-viewing radiometers is β , the angle between the orbit plane and a vector to the Sun. GACM's orbit, at 52° inclination, precesses so that the SMLS sees β angles in the range $\pm 75^\circ$. The mission is assumed to include yaw maneuvers as required to avoid sunlight on one face of the spacecraft bus used for thermal control of the front end electronics. Two orbit simulation programs, one stand-alone and one built in to the thermal model, were used to find the times when solar illumination of the SMLS antenna would be extreme and to identify worst-case orbit times for further analysis. Fig. 1a shows the solar illumination of the SMLS at this worst-case orbital β angle and time, which was used for the subsequent structural and optics analyses. The worst-case time and pixel are determined more by self-shadowing of the

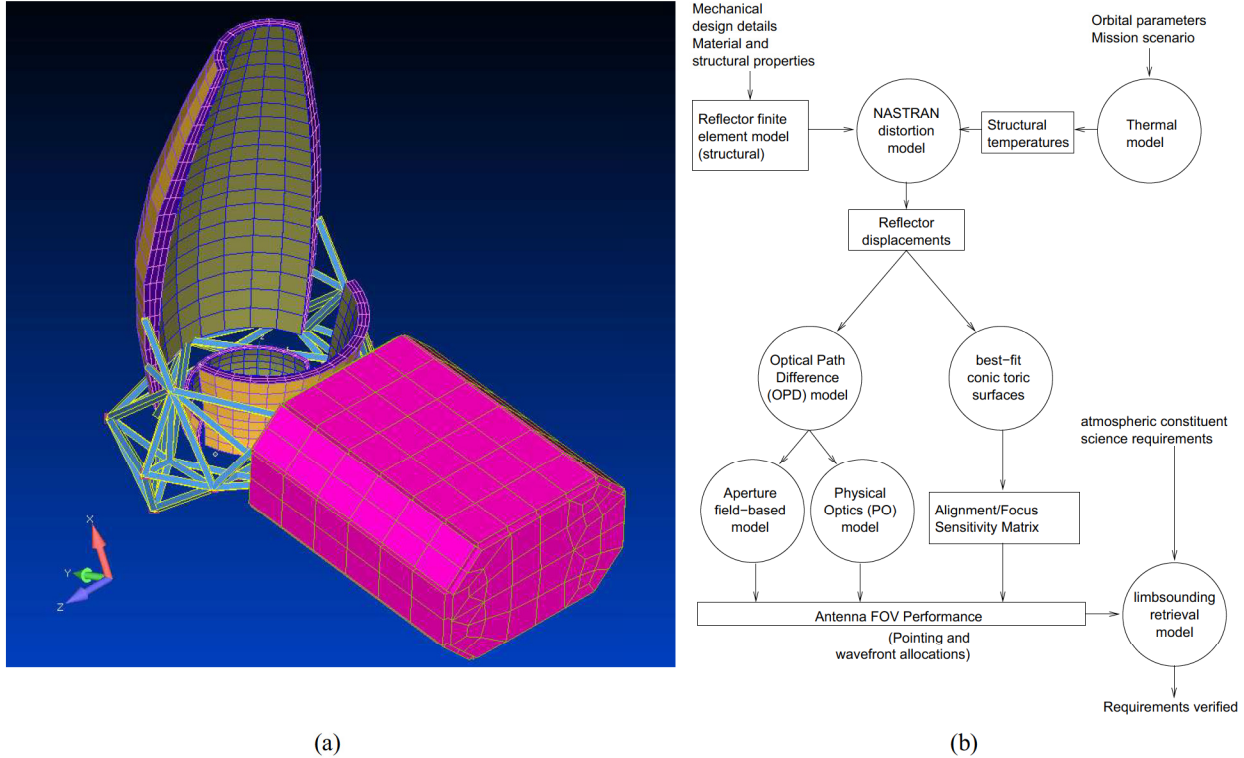


Figure 2. SMLS math models: (a) I-DEAS finite element model of antenna with notional spacecraft bus; and (b) data flow through thermal, structural, optical and geophysical retrieval models.

reflector (one edge misses shading the other from direct sunlight but blocks half the solid angle for re-radiation of heat, in contrast to the center pixel) than by entry/exit of Earth’s shadow.

Thermal, structural and optical models have been maintained and refined since earlier studies showed feasibility of a composite architecture for the 4 m SMLS antenna. The models include primary, secondary and tertiary reflectors, support structure and a notional spacecraft bus. The SMLS reflector geometry was modeled using the I-DEAS CAD environment and material properties which Vanguard provided. Finite element grids were generated for thermal and structural models. These two models share a common mesh, shown in Fig. 2, to eliminate temperature mapping when converting the thermal model predictions to structural model thermal loads. The grid resolution was chosen for reasonable element sag and aspect ratio, given that the core would be modeled using equivalent bulk properties, rather than a detailed egg-crate structure. We justify this approximation for SMLS from experience with EOS MLS, which showed good agreement between the bulk model and the vendor’s high resolution model, for the modest requirements of an antenna system operated at sub-mm wavelengths.

The grid spacing used for evaluating optical performance is defined by the area of the primary reflector which is illuminated at each azimuth pixel, and is 2–4× finer in each direction than the thermal/structural grid. Therefore, the optics model can use the full spectrum of spatial structure available in its input data. This will become important when a future structural model is refined to incorporate the details of the egg-crate structure. In this “print-through” phenomenon, the unsupported front skin between core ribs leads to dimples in the reflecting surface.

The antenna system was modeled in Code V[®], a proprietary optical analysis program developed by Optical Research Associates, a subsidiary of Synopsis, Inc. First, a ray-trace model was developed for the center pixel of SMLS in receive mode, as described elsewhere¹ Fig. 3 shows the exit pupil map of this system for the nominal Gaussian illumination of a single pixel. The intensity map is similar to the Tertiary Reflector surface current map¹ from a Physical Optics (PO) calculation for the earlier version of SMLS in transmit mode. The agreement

in shape validates the Code V model and confirms that the antenna transforms a Gaussian beam of high aspect ratio to a nearly axisymmetric beam compatible with the feed optics.

As is typical for microwave optical systems having large numerical aperture (small f/D), pupil distortion is evident in the intensity and especially the wavefront map. Although Code V has the capability to apply NASTRAN deformations to optical surfaces, we found the phase variation was large enough that peripheral rays frequently fall outside the bounding boxes needed to define the subsequent toric surfaces (Secondary and Tertiary). Therefore, a better approach is to model the antenna as a transmitter. Not only does this correctly model the illumination pattern of the radiometer feed, resulting in a field distribution in the aperture which can be transformed to the far zone and convolved with the Earth limb radiance, but the primary's thermal deformations now occur on the last finite surface, and ray failures at the inner apertures are less frequent. This methodology has been used for many previous reflector antenna systems,³ including the UARS and EOS MLS precursors to SMLS, and is consistent with the PO model shown in Fig. 2b.

When modified for transmit mode, the Code V model predicts that aperture fields for the undeformed case have peak phase errors ($\sim \pm\lambda/20$) consistent with Fig. 3b. The thermal deformations result in additional phase errors $\sim \pm\lambda/8$, which have been matched for a few cases to the receive-mode model. However, for quick results, a simpler model (easier to evaluate for all azimuth pixels and separable for any subset of antenna reflectors) was constructed using software developed for the previous MLS optics. At each node for which thermal deformations were provided, the simplified model evaluates the Optical Path Difference (OPD):

$$\text{OPD} = -2\hat{n} \cdot \vec{\delta} \cos \theta_i,$$

where \hat{n} , $\vec{\delta}$, and θ_i are the surface normal, translational component of deformation, and ray incidence angle, respectively, at the reflection point. Rotational components of deformation are not used, but are assumed to be consistent with the distribution of individual translations. That is, for each ray we calculate a phase change modeled by a piston component, and assume that the phase tilt and curvature are adequately described by spatial derivatives of the piston field. For sufficiently small deformations, the transmit FOV pattern can then be estimated by combining the OPD distribution as a phase error function with the nominal aperture amplitude.

The SMLS antenna differs from its predecessors in that a given element of surface area on each reflector affects several adjacent azimuth pixels. Thus we calculate OPD in two ways: first, given the arrangement of nodes in azimuth pixels (each several nodes long *per* Fig. 2), calculate OPD at each node using the ray parameters for the pixel centered on that node. Second, for each pixel, calculate an OPD map which matches the previous calculation along the center line but uses the paraxial ray behavior (cylindrical wavefront incident from the limb) in the azimuth direction. As noted above, the illumination half-width is 2–4 \times smaller than the grid size, so this requires interpolation from just the two adjacent node lines.

The first method gives the registration between all azimuth pixels, while the second determines the FOV shapes of each pixel, which we characterize relative to the undeformed pixel using the 5 lowest moments (piston, V and H tilt, and V and H curvature) of the aperture (near) field. The SMLS detectors do not record the relative phases of adjacent pixels, so we discard the piston.

To assess whether the far field patterns of SMLS meet GACM science requirements we must convolve them with radiances from Earth's limb provided by a forward model⁴ We calculate patterns using a PO model based on reflector geometry and feed pattern characteristics. Fig. 4a shows a forward raytrace through the PO model (the reflectors extend beyond where the surface currents of a single pixel drop to near zero), and principal plane cuts of the far-field pattern. In addition to the 20:1 beam aspect ratio due to the toric design, these patterns in Fig. 4b show the sidelobe asymmetry corresponding (by reciprocity) to the pupil distortions of Fig. 3. Like its ray-optical counterpart, the PO model can be used to predict beam degradation by applying modeled or measured surface distortions to the reflecting surfaces.

We used the thermal/structural/optical models to predict FOV performance at several solar β angles, for enough orbits to extinguish start-up transients and in both forward and backward flight directions to account for yaw maneuvers. We varied absorptivity and emissivity over ranges consistent with the EOS MLS design to develop sensitivity, as well as several choices of paint or grit blasting of the active surface; multi-layer insulation

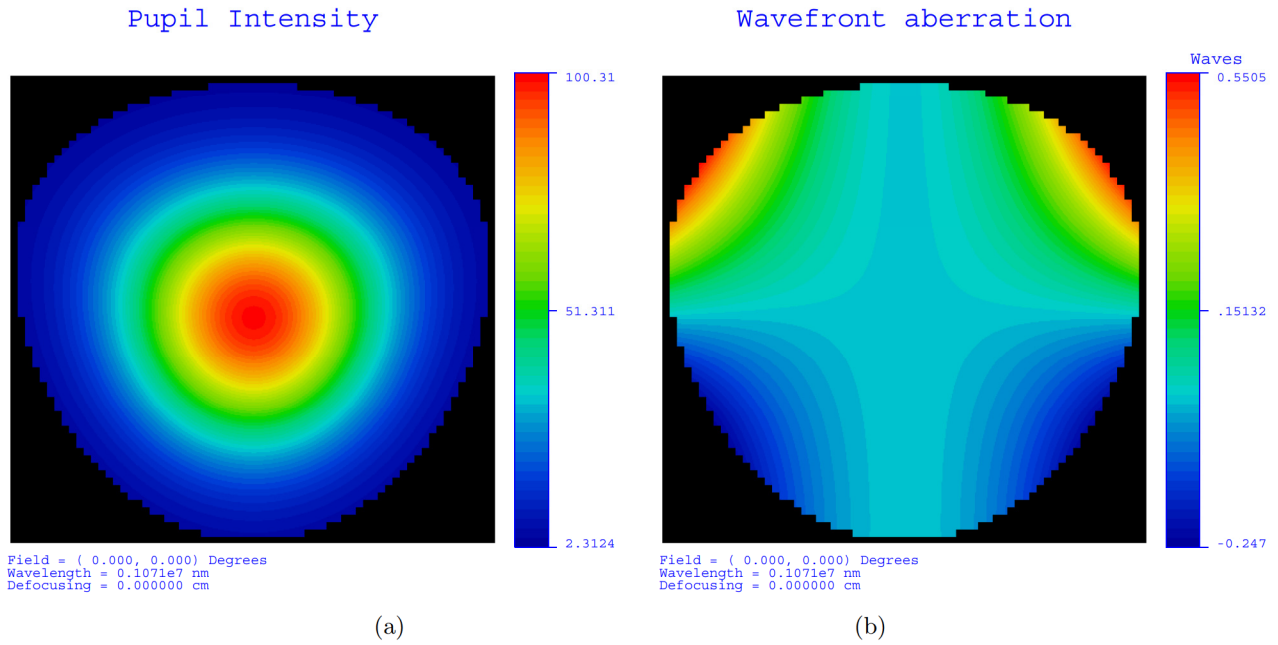


Figure 3. Exit pupil map for undistorted SMLS receive mode: (a) intensity and (b) phase at 280 GHz.

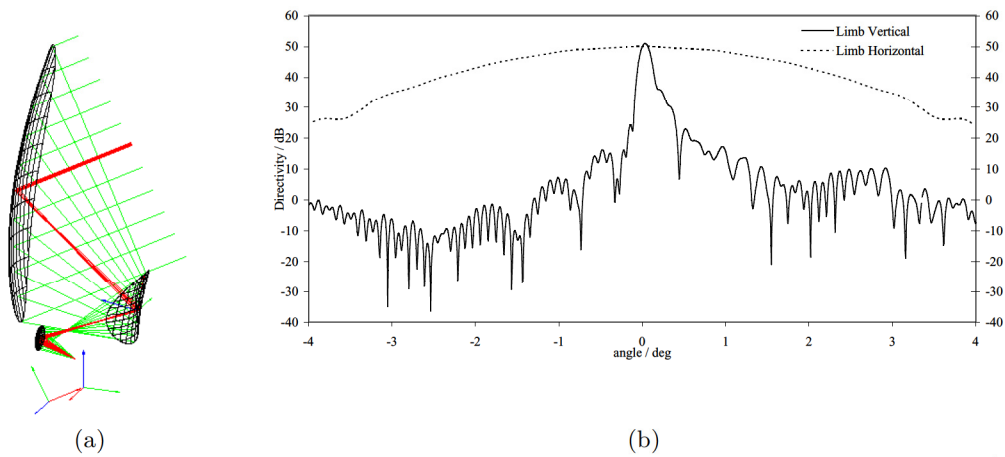


Figure 4. SMLS FOV models: (a) GRASP physical optics model showing principal ray fans, and (b) far-field patterns scaled from a previous SMLS design.¹

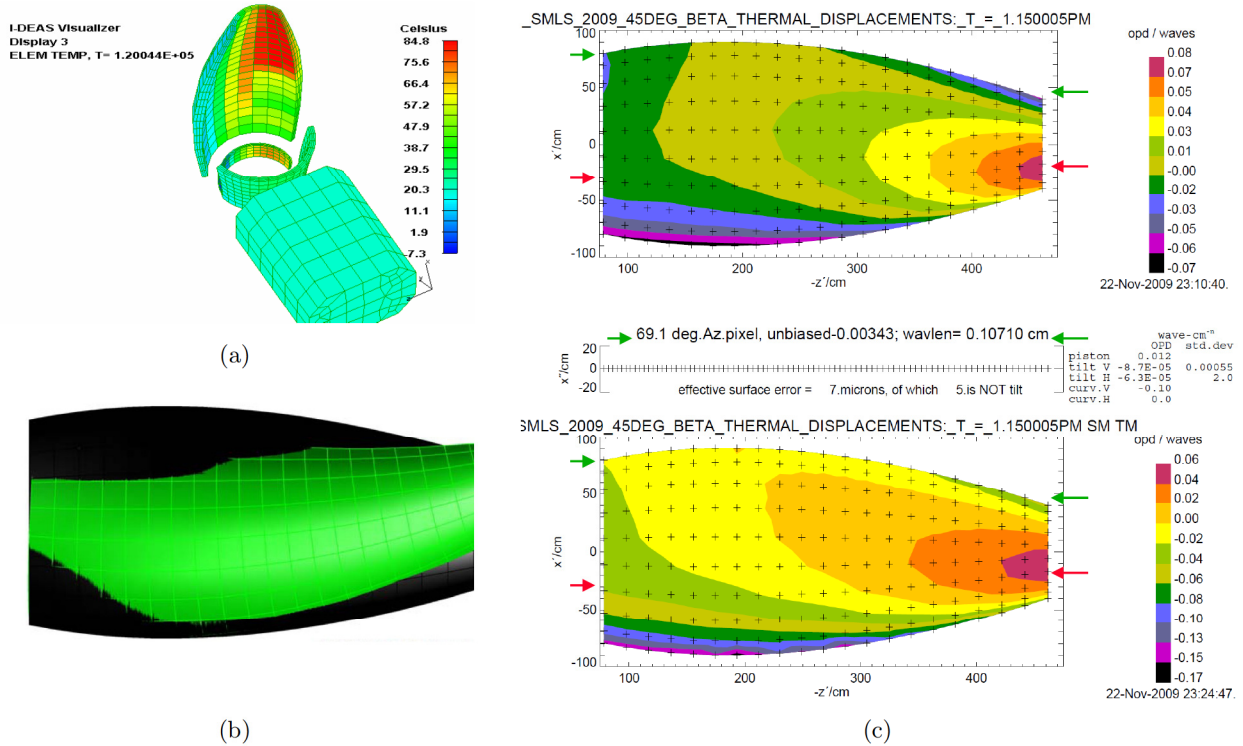


Figure 5. Thermal/Structural/Optical model predictions at worst-case time in orbit of Fig. 1: (a) temperature fields; (b) corresponding distortion of Primary Reflector predicted from NASTRAN model, exaggerated 5000 \times ; and (c) OPD maps for Primary alone (top) and for all 3 antenna reflectors (bottom)

was simulated on back surfaces and structure. Finally, we varied material properties (CTE and thermal conductivity) and core thickness to check out our model; these steps were also done by Vanguard, using a more detailed composite model, in design iterations for the reflector fabrication described below.

Fig. 5 shows results for the worst-case orbit and time, with material properties provided by Vanguard. The magnitude of temperature gradient is roughly comparable to what was predicted for and experienced by Aura MLS in its 705 km sun-synchronous orbit. The figure also shows the corresponding distortion of the Primary Reflector, and OPD maps for the Primary alone and for the complete antenna; these two cases show that, as for Aura MLS, the Primary contributes 70–80% of total distortion and hence dominates the overall optical performance. Although it exceeds distortions predicted for Aura MLS, the OPD range of $\pm 0.1\lambda$ at 280 GHz is probably tolerable, while performance at 680 GHz will likely require adjustments (typically table-driven and obtained from pre-launch calibration) to patterns used in orbit.

3. FABRICATION AND TEST

3.1 Demonstration Primary Reflector

Following the success of JPL’s Aura MLS (operating from 118 to 660 GHz),⁵ we designed, fabricated and tested a demonstration primary using SBIR and Earth Science Technology Office (ESTO) funding. This reflector has an all-composite architecture with egg-crate core and front and rear face skins, to meet a total surface error budget of 12 μm rms. We identified key material properties, notably near-zero in-plane face skin and core laminate CTE, and thermally conductive core laminate technology, achieved through pre-preg selection, tuning of materials, and standard lay-up and curing processes. Both the segmented core ribs and faceted back skin are planar elements to simplify design, analysis and assembly while maintaining low parasitic mass and high fundamental resonant frequency. For the core laminate, mesh was embedded in composite to reduce thermal strain. Both front and rear skins were tiled to improve isotropy of material properties, especially CTE.

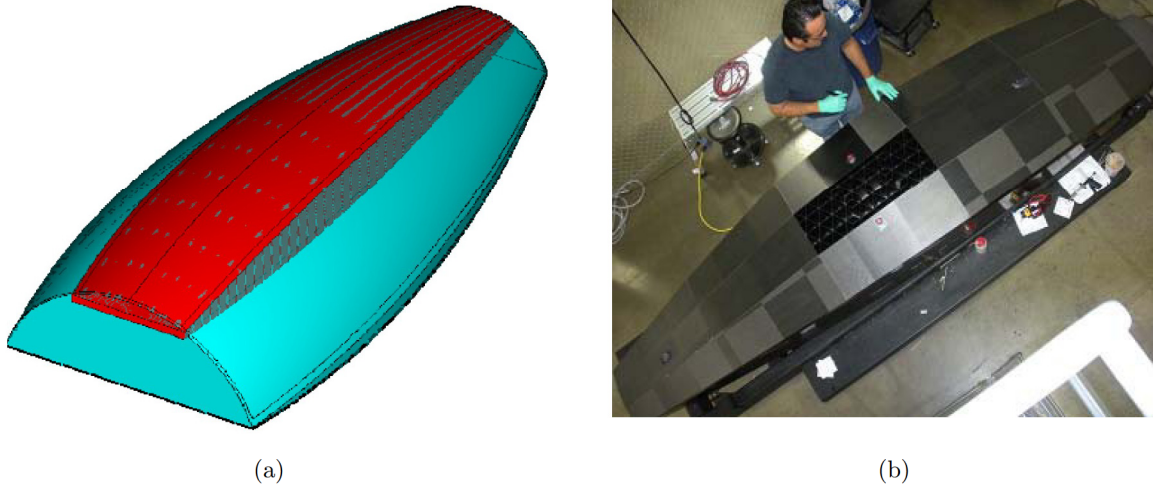


Figure 6. Fabrication of demonstration primary: (a) reflector mold, comparing center third used in the SBIR (red) to full width for GACM (blue); and (b) installation of back skin facets over core in the SBIR reflector inverted on its mold.

To fit within the resources of an SBIR program, we determined that the critical parts of the toric primary design could all be met with a demonstration reflector of the full 4 m height but only 1/3 the width. Fig. 6 shows the 1/3×full-height mold concept and a photograph of the latter stages of the demonstration reflector assembly with the core structure still visible before installation of the last back skin facet.

We also relaxed the GACM SMLS surface accuracy requirement ten-fold, to 120 μm rms, and separated the thermal stability requirement from the total accuracy budget (*i.e.*, even with as-built figure errors much larger than a flight SMLS could tolerate, the thermal deformations we could measure would accurately indicate the thermal stability of the flight article). Surface accuracy of the mold delivered to Vanguard was 24 μm rms, *i.e.* 1/5 the specification but still 7 times more than GACM SMLS will allow for the mold.

In current research, Vanguard has identified improvements in mold fabrication, mold machining to the tolerances SMLS will require, and metrology of both the improved mold and the replicated reflector. We anticipate that in current or future development, these improvements will allow replication of full width face skins, meeting SMLS requirements, from a monolithic mold.

3.2 Thermo-Elastic Distortion (TED) test

3.2.1 Configuration and initial results

Thermal stability of the demonstration reflector in air was tested over several days in a chamber at Wyle Labs. Test methodology followed that of Thermo-Elastic Distortion (TED) tests performed on many previous Vanguard communications antennas. The profile began with a 6-hour dry-out at 90°C followed by holds, typically 1 hour long, at plateaus down to -120°C. At each plateau we took photogrammetry measurements, rotating the reflector and using dual camera viewports to develop 3-D data sets. Fig. 7 shows the reflector configured for test and the temperature profile.

The photogrammetric bundling accuracy ranged from 8 to 15 micron at the hot and cold extrema, respectively, indicating measurement accuracy comparable to other reflector tests. The SBIR final report² contains surface distortion maps at the temperature plateaus; *e.g.* rms residuals from best-fit focal lengths are 38 micron at ambient and 28 micron at -100°C. That report also gives a factor of 6.8 (for the 830 km orbit) by which the *specific change in surface accuracy* (units of μm rms/°C) should be scaled to infer orbital performance from TED test deformations. Since the current goal for SMLS allows 3 micron rms of error due to 28–51° C range (*i.e.* 0.059–0.11 micron rms /° C), we deem the design associated with the 1.6 micron rms prediction due to -120° C (*i.e.* 0.13 micron rms /° C) is acceptable from a thermal distortion perspective.

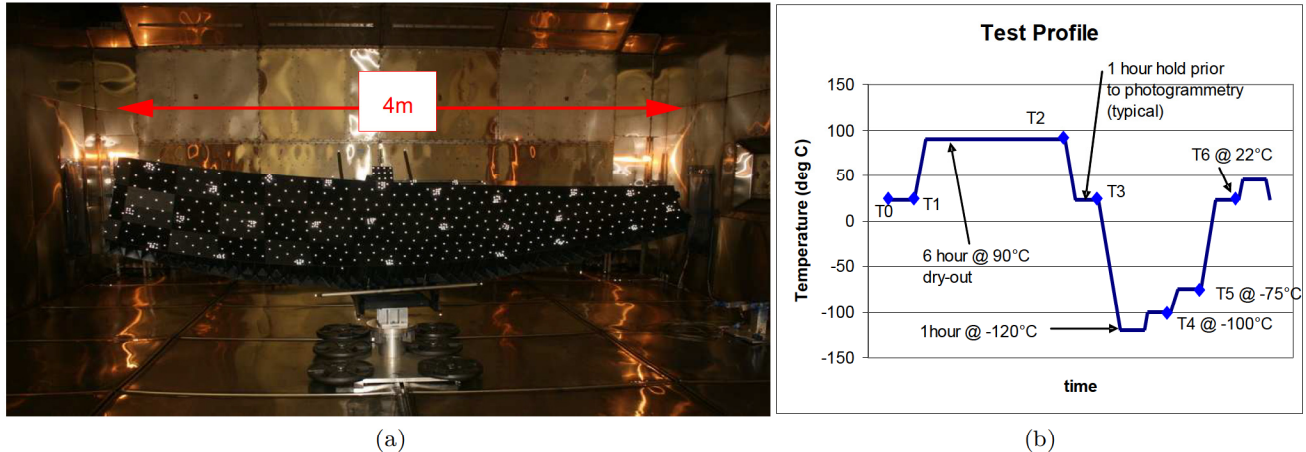


Figure 7. Thermal soak test: (a) Demonstration reflector with photogrammetry targets in test chamber, and (b) temperature profile.

3.2.2 Correlation with FEM prediction

Fig. 8 shows preliminary results from current studies to refine the correlation between TED measurements and distortions predicted by the Finite Element Models. The full-width primary reflector model was extracted from the orbital performance models, reduced in width to match the SBIR demonstration model, and subjected to 1G, moisture dryout and isothermal soak loads, using the support boundary conditions of the TED test. The figure compares predicted OPD maps with those measured at ambient, hot (+90° C) and cold (-100° C) plateaus (OPD is relative to the nominal prescription for the ambient case, and relative to ambient for the other 2 plateaus). RMS and peak OPDs, as well as contours, match those obtained by measurements of the mold and replicated reflector within reasonable levels, but further study of the temperature cases is needed, since the observed OPDs are opposite those predicted using putative material properties for the reflector. Given that the design called for near-0 coefficient of thermal expansion (CTE) of the laminates, this initial result is not worrisome. Along with adjusting thermal expansion and conductivities to study this difference, we will have material properties of witness coupons measured as part of the current research.

4. CURRENT AND FUTURE WORK

Development of the SMLS antenna continues under an Instrument Incubator Program administered by ESTO. Results from the TED correlation described above will be fed back into Vanguard’s reflector design, with the intention to produce a full width primary reflector having surface accuracy improved toward the 680 GHz requirements of GACM SMLS. We are also developing thermal gradient tests to be performed in a large facility at JPL, simulating the orbital environment and measuring distortions with improved metrology techniques. These are based on speckle interferometry of the reflector surface, plus laser ranging metrology sensors at selected test points around the aperture. We are incorporating model predictions into geophysical retrieval models developed by the MLS science team, to assess in-orbit performance. Finally, we plan to fabricate a breadboard antenna, combining the composite primary with other reflectors and with feed systems developed under a related Instrument Incubator Program. We will then measure beam patterns of the assembly on a Near Field Range at JPL.

5. SUMMARY

The toric Cassegrain concept for the SMLS antenna provides significant enhancements to limb sounding of the lower stratosphere and upper troposphere in the sub-mm and far IR regimes. Recent and current research programs have identified challenges and found solutions for the optical performance in thermal orbital environments, and we expect that SMLS will continue to meet atmospheric science requirements, as did its predecessors, while maintaining the added benefits of resolution and coverage.

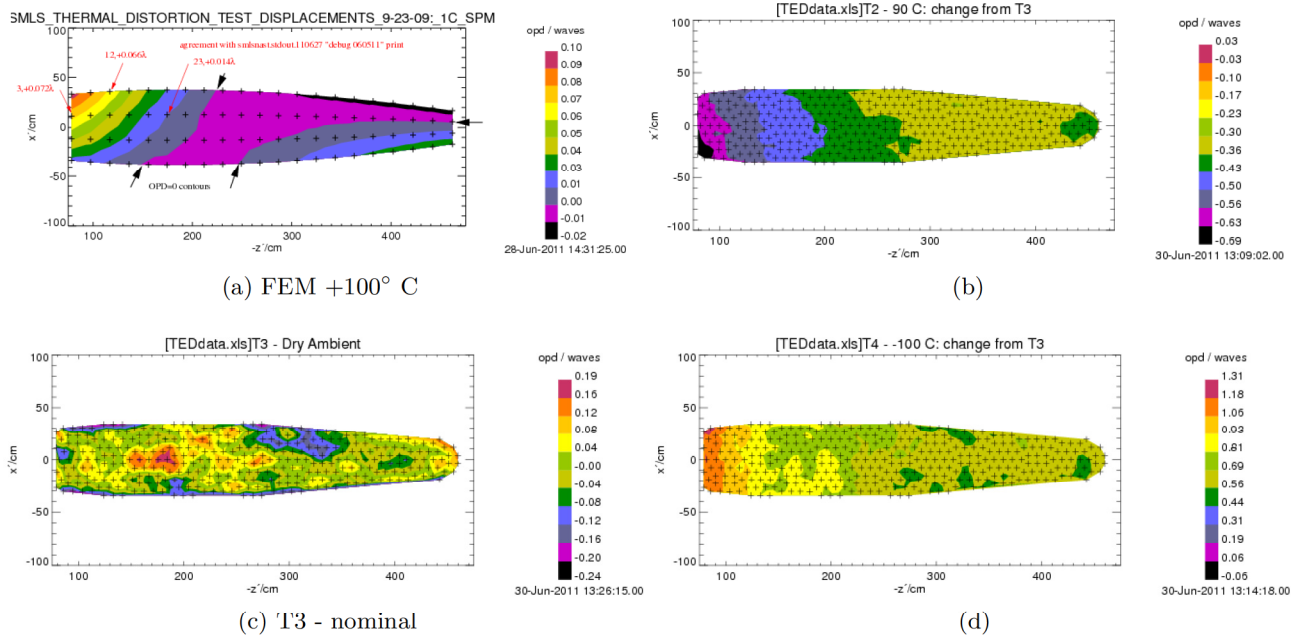


Figure 8. OPD maps of demonstration reflector in thermal soak configuration: (a) Finite Element Model prediction for $\Delta T = +100^\circ \text{C}$; photogrammetric measurements (b) (dry ambient plateau) - (nominal); (c) $+90^\circ \text{C}$ - ambient; and (d) -100°C - ambient.

ACKNOWLEDGMENTS

We gratefully acknowledge contributions by many colleagues, especially: Dr. E. Cohen for expertise in the application of composite reflector technology to large-aperture systems, applied in numerous areas to this research; Dr. P. Stek for supporting SMLS instrument development; Mr. J. Waldman and Mr. E. Kwack for creating the mechanical and thermal models and generating the temperature and deformation fields; and Mr. M. Miller for breadboard reflector engineering and mathematical modeling. This work was performed by the Jet Propulsion Laboratory, California Institute of Technology, under contract with the National Aeronautics and Space Administration. Copyright 2011. All rights reserved.

REFERENCES

- [1] Cofield, R. E., Cwik, T. A., and Raouf, N. A., "Toric offset three-reflector antenna for an advanced microwave limb sounder," in [*Highly Innovative Space Telescope Concepts, Proceedings of SPIE, 4849*], (August 2002).
- [2] Kasl, E. P., "Lightweight Thermally Stable Multi-Meter Aperture Submillimeter Reflectors," tech. rep., DR Technologies, Inc. (2010). Phase II SBIR Final Report.
- [3] Imbriale, W. A. et al., "Instrument packages," in [*Spaceborne Antennas*], ch. 7, JPL DESCANSO Monograph Series (2006). ISBN: 0470051507.
- [4] Read, W. G. et al., "The Clear-Sky Unpolarized Forward Model for the EOS Aura Microwave Limb Sounder," *IEEE Transactions on Geoscience and Remote Sensing* **44**, 1367–1379 (May 2006).
- [5] Cofield, R. E. and Stek, P. C., "Design and Field-of-View Calibration of 114–660 GHz Optics of the Earth Observing System Microwave Limb Sounder," *IEEE Transactions on Geoscience and Remote Sensing* **44**, 1166–1181 (May 2006).